Cell. Mol. Life Sci. (2012) 69:2791–2803
DOI 10.1007/s00018-012-0955-z

Cellular and Molecular Life Sciences

RESEARCH ARTICLE

Chromogranin A binds to αvβ6-integrin and promotes wound healing in mice

Flavio Curnis · Anna Maria Gasparri · Renato Longhi · Barbara Colombo · Silvia D'Alessio · Fabio Pastorino · Mirco Ponzoni · Angelo Corti

Received: 28 September 2011 / Revised: 7 February 2012 / Accepted: 27 February 2012 / Published online: 14 March 2012

Abstract Chromogranin A (CgA), a secretory protein expressed by many neuroendocrine cells, neurons, cardiomyocytes, and keratinocytes, is the precursor of various peptides that regulate the carbohydrate/lipid metabolism and the cardiovascular system. We have found that CgA, locally administered to injured mice, can accelerate keratinocyte proliferation and wound healing. This biological activity was abolished by the $Asp_{45}Glu$ mutation. CgA and its N-terminal fragments, but not the corresponding $Asp_{45}Glu$ mutants, could selectively recognize the αvβ6-integrin on keratinocytes (a cell-adhesion receptor that is up-regulated during wound healing) and regulate keratinocyte adhesion, proliferation, and migration. No binding was observed to other integrins such as αvβ3, αvβ5, αvβ8, α5β1, α1β1, α3β1, α6β4, α6β7 and α9β1. Structure–activity studies showed that the entire $CgA_{39–63}$ region is crucial for αvβ6 recognition ($K_i = 7$ nM). This region contains an RGD site (residues $CgA_{43–45}$) followed by an amphipathic α-helix (residues $CgA_{47–63}$), both crucial for binding affinity and selectivity. These results suggest that the interaction of the RGD/α-helix motif of CgA with αvβ6 regulates keratinocyte physiology in wound healing.

Keywords Chromogranin-A · Vasostatin-1 · αv/β6 Integrin · Wound healing

Abbreviations

CgA	Chromogranin-A
hCgA	Human CgA
rCgA	Recombinant CgA
VS-1	Vasostatin-1
STV	Streptavidin
HRP	Peroxidase

Introduction

Chromogranin A (CgA) is a secretory protein expressed by many normal and neoplastic neuroendocrine cells, neurons, cardiomyocytes, granulocytes, and keratinocytes [1–3]. This protein, 439 residues long, may function as a precursor of biologically active peptides that are involved in the regulation of vascular tension, heart contractility, innate immunity, carbohydrate and lipid metabolism, angiogenesis and tumor physiology [1, 2]. For example, CgA can give rise, upon cleavage, to pancreastatin, a CgA250–301 fragment involved in the regulation of carbohydrate and lipid metabolism [4, 5], or to catestatin ($CgA_{352–372}$), a fragment that regulates catecholamine secretion and that has a role as a regulator of the cardiovascular system [6–8].

Electronic supplementary material The online version of this article (doi:10.1007/s00018-012-0955-z) contains supplementary material, which is available to authorized users.

F. Curnis · A. M. Gasparri · B. Colombo · A. Corti (✉)
Division of Molecular Oncology and IIT Network Research Unit of Molecular Neuroscience, San Raffaele Scientific Institute, via Olgettina 58, 20132 Milan, Italy
e-mail: corti.angelo@hsr.it

R. Longhi
Istituto di Chimica del Riconoscimento Molecolare, CNR, 20131 Milan, Italy

S. D'Alessio
Division of Genetics and Cell Biology, San Raffaele Scientific Institute, 20132 Milan, Italy

F. Pastorino · M. Ponzoni
Laboratory of Oncology, Experimental Therapy Unit, G. Gaslini Children's Hospital, 16148 Genoa, Italy

Cleavage of CgA can also give rise to vasostatin-1 ($CgA_{1–76}$), a fragment that regulates vascular tension [1], heart contractility [9], and native immunity [1, 10]. Thus, intra-granular and/or extracellular proteolytic processing of CgA, e.g., by prohormone convertase 1 and 2, furin, plasmin, and cathepsin L [11–14], is an important mechanism for regulating its biological activity.

We have previously shown that CgA can also inhibit the adhesion of fibroblasts to various extracellular-matrix proteins, whereas the $CgA_{1–78}$ fragment (VS-1) can promote cell adhesion and spreading [15–18]. CgA and VS-1 can also enhance endothelial cell–cell adhesion and protect the endothelial barrier integrity from vascular leakage induced by tumor necrosis factor alpha [19, 20]. Furthermore, VS-1 can inhibit VEGF induced endothelial cell proliferation and migration [21]. The receptors that mediate the biological effects of CgA and its fragments in cell adhesion, migration and proliferation are still unknown.

The present study was undertaken to investigate whether CgA might recognize integrins, a family of membrane receptors typically involved in the regulation of cell adhesion, proliferation, and migration [22, 23]. These receptors are made of different combinations of α and β subunits [23]. Given that a subset of integrins, such as αIIbβ3, α5β1, α8β1, αvβ1, αvβ3, αvβ5, αvβ6 and αvβ8, can recognize the sequence Arg-Gly-Asp (RGD) in a variety of different substrates [23, 24] and that this motif is present also in CgA, we have studied the interaction of CgA with this subclass of receptors. We show that the RGD sequence of CgA ($CgA_{43–45}$) and the adjacent amphipathic α-helix (residues $CgA_{47–63}$) form a site that selectively and efficiently recognize the integrin αvβ6, a receptor that is up-regulated in keratinocytes and other epithelial cells during tissue remodeling, wound healing, and carcinogenesis [25]. Furthermore, we show that RGD-dependent interactions between CgA and integrins can regulate keratinocyte adhesion and accelerate wound healing in a mouse model.

Materials and methods

Cell lines, antibodies, and reagents

Human skin keratinocytes cells (HaCaT) were kindly provided by Dr. Boletta Alessandra (San Raffaele Scientific Institute, Italy). Normal human dermal fibroblasts (HDFa) were from American Type Culture Collection (ATCC, Manassas, VA); human endothelial cell fused with human lung carcinoma A549 cells (EA.hy926) were described previously [26]. These cells were cultured in DMEM containing 10 % fetal bovine serum, 50 µg/ml streptomycin sulfate, and 100 U/ml of penicillin. Mouse skin keratinocytes were prepared as described [27]. Other reagents were: anti-human CgA monoclonal antibodies (mAbs) 5A8, 7D1, B4E11, and A11, produced and characterized as described previously [16, 28]; anti-αvβ6 mAb 10D5 (Millipore, Billerica, MA) and anti-α6 mAb 135-13C (Immunological Sciences, Rome, Italy); anti-$CgA_{410–439}$ rabbit polyclonal antibody (Primm, Milan, Italy); anti-keratin 14 rabbit polyclonal antibody (AF64, Covance, Princeton, NJ); anti-Ki67 rabbit polyclonal antibody (Novo Castra); Alexa-Fluor-conjugated goat anti-rabbit IgG secondary antibody (488 and 546 nm, Invitrogen); human α5β1, αvβ3, αvβ5 integrins (Immunological Sciences); recombinant human αvβ6, αvβ8, α1β1, α1β3, α6β4, α6β7 and α9β1 integrins (R&D System, Minneapolis, MN).

Preparation of CgA, CgA fragments, peptides, and muteins

Human recombinant chromogranin A (rCgA) was expressed in *E. coli* and purified by ion exchange chromatography using a Q-Sepharose Fast Flow column (GE Healthcare, UK), followed by dialysis against 20 mM Tris–HCl pH 7.5, 1 mM $CaCl_2$, 0.1 M KCl. The product was purified by affinity chromatography using a calmodulin–agarose column (Sigma-Aldrich, St. Louis, MO), diluted in 20 mM Tris–HCl, 1 mM EDTA, pH 8, and purified by ion exchange chromatography using a Source 15Q column (GE Healthcare, UK). The sample was de-pyrogenated using AffinityPak Detoxy-Gel Endotoxin Removing Gel (Thermo Scientific, MA) and characterized by SDS-PAGE, ELISA, and mass spectrometry. The product was homogeneous and its purity was >95 % as estimated by SDS-PAGE analysis (Fig. 1a, inset) and Western blot (not shown). The rCgA $Asp_{45}Glu$ mutant (called rCgA–RGE), was prepared by recombinant DNA technology as described for rCgA (Fig. 1a, inset). Recombinant vasostatin-1 (VS-1, corresponding to STA–CgA1–78) and natural human CgA (CgA) were prepared as described [29]. Various CgA peptide fragments (Supplementary Table 1S) were synthesized by the solid-phase Fmoc method [30]. All peptides were dissolved in water and stored in aliquots at –20 °C. The molecular mass of each peptide was checked by MALDI-TOF mass spectrometry analysis.

Direct binding assay of CgA and VS-1 to integrins

Integrin solutions (1–0.5 µg/ml) in phosphate-buffered saline with Ca^{2+} and Mg^{2+} (DPBS, Cambrex) were added to 96-well polyvinylchloride microtiter plates (50 µl/well, Falcon 3912, Becton–Dickinson) and left to incubate overnight at 4 °C. All subsequent steps were carried out at room temperature. The plates were washed with DPBS and further incubated with DPBS containing 3 % BSA (200 µl/well, 1 h). After washing with 25 mM Tris–HCl, pH 7.4,

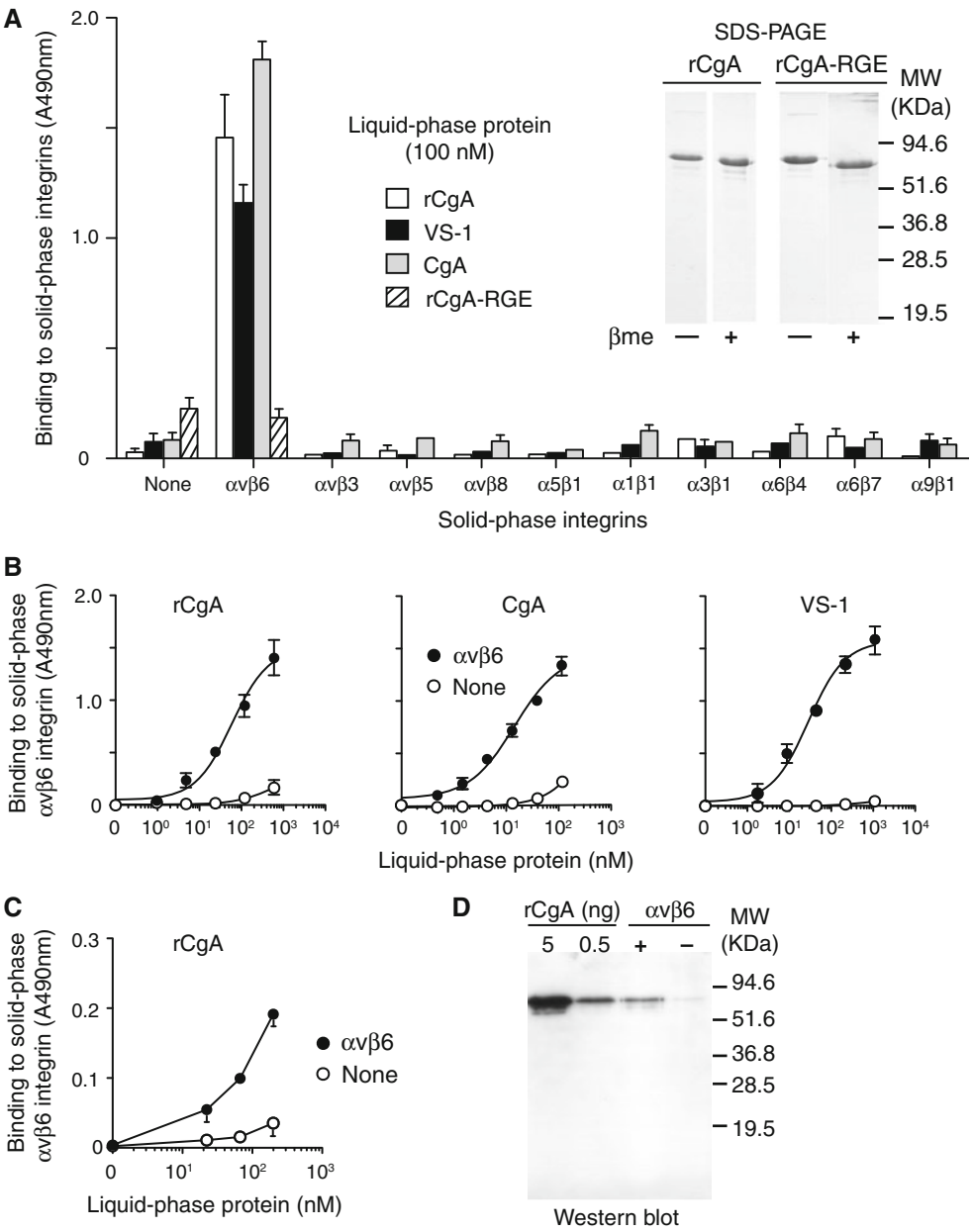

Fig. 1 Both full-length CgA and its N-terminal fragment VS-1 selectively binds to $\alpha v\beta 6$-integrin. **a–c** Binding of natural and recombinant CgA (CgA and rCgA, respectively) and vasostatin-1 (VS-1) to integrins adsorbed onto microtiter plates. Binding was detected using the anti-CgA mAb B4E11 (epitope CgA 68–71) (**a**, **b**) or using a rabbit polyclonal anti-$CgA_{410–439}$ (**c**) followed by a goat anti-mouse or -rabbit IgG-peroxidase conjugates. A representative experiment of three independent experiments (each in duplicate) is shown (mean ± SE). **a** *Inset* SDS-PAGE analysis of rCgA and $Asp_{45}Glu$ mutant (rCgA–RGE) under reducing and non-reducing conditions. **d** Western-blot analysis with mAb B4E11 of the $\alpha v\beta 6$-coated plates incubated with rCgA confirms that full-length CgA can bind to $\alpha v\beta 6$

containing 150 mM sodium chloride, 1 mM magnesium chloride, and 1 mM manganese chloride (buffer A) the plates were filled with chromogranin A or VS-1 solution (50 µl/well) in buffer B (buffer A containing 1 % BSA and 0.05 % Tween 20) and left to incubate for 2 h. After washing with buffer A containing 0.05 % Tween 20, each well was incubated with mAb B4E11 in buffer B (5 µg/ml, 50 µl/well, 1 h) followed by a goat anti-mouse peroxidase conjugate in the same buffer (diluted 1:1,000, 50 µl/well, 1 h). Bound peroxidase was detected by adding *O*-phenylenediamine chromogenic substrate (70 µl/well).

Competitive binding assays

A complex made of biotinylated acetyl-C*iso*DGRCGVR SSSRTPSDKY peptide with a streptavidin-peroxidase conjugate (*iso*DGR–STV/HRP) was prepared as described previously [31]. This complex was diluted with buffer B (without Tween-20), and mixed with various amounts of proteins or peptides. The mixtures were then added to microtiter plates coated with integrins and incubated for 2 h at room temperature. After washing the bound peroxidase was detected as described above.

Preparation of $CgA_{38–63}$-Qdot

Amine-modified Qdot nanoparticles (2 nmol of Qdot605 ITK Amino (PEG), Invitrogen, Carlsbad, CA) were activated with sulfosuccinimidyl 4-[*N*-maleimidomethyl] cyclohexane-1-carboxylate (Sulfo-SMCC; Pierce, Rockford, IL), a heterobifunctional crosslinker, according to the manufacturer's instructions. The maleimide-nanoparticles were purified from unreacted crosslinker by gel-filtration chromatography on NAP-5 column (GE Healthcare). The product (200 µl) was mixed with $CgA_{38–63}$ or $CgA_{38–63}$ (RGE) (160 µg in 32 µl of water) or with water and incubated for 2 h at room temperature. 2-mercaptoethanol was then added (0.1 mM final concentration) and left to incubate for 0.5 h at room temperature. The conjugates [called $CgA_{38–63}$-Qdot, $CgA_{38–63}$(RGE)-Qdot and Qdot] were separated from free peptide by ultrafiltration using Ultra-4 Ultracel-100 K (Amicon), resuspended in 100 mM Tris–HCl, pH 7.4, containing 0.02 % sodium azide, and stored at 4 °C.

Binding assay of $CgA_{38–63}$-Qdot to human keratinocytes

Binding assays of $CgA_{38–63}$-Qdot, $CgA_{38–63}$(RGE)-Qdot or Qdot were carried out as follows: human keratinocytes cells (HaCaT) were grown in chamber slides (7×10^4 cell/well). The cells were washed with 25 mM HEPES buffer, pH 7.4, containing 150 mM sodium chloride, 1 mM magnesium chloride, 1 mM manganese chloride (called "buffer C") and incubated with $CgA_{38–63}$-Qdot, $CgA_{38–63}$(RGE)-Qdot or Qdot solution (1:30 in buffer C, containing 1 % BSA, called "buffer D") for 2 h at 37 °C, 5 % CO_2. The cells were washed again with buffer C, fixed with paraformaldehyde for 20 min, counterstained with DAPI (Invitrogen), and analyzed using fluorescence microscopy. FACS analysis was carried out as follows: HaCaT cells were detached with trypsin/EDTA solution. After washing with DPBS, the cells were resuspended in buffer D containing $CgA_{38–63}$-Qdot or Qdot (1:30 dilution, 5×10^5 cell/100 µl tube) and left to incubate 2 h at 37 °C. After washing with buffer C, the cells were fixed with formaldehyde and analyzed using the LRS-II flow cytometer (Becton–Dickinson, equipped with 605WB20 emission filter, Omega Optical).

Cell adhesion assays

Cell-adhesion assays were carried out using 96-well polyvinyl chloride microtiter plates (Falcon 3912) coated with various proteins (10 µg/ml in 0.15 M sodium chloride, 0.05 M sodium phosphate buffer, pH 7.3, 50 µl/well, 16 h, 4 °C). After washing with 0.9 % sodium chloride solution, the plates were blocked with 3 % bovine serum albumin (BSA) solution in DMEM and further incubated for 1 h at room temperature. The plates were then filled with HaCaT cell suspension (70,000/well), with or without competitor peptides, in DMEM containing 0.1 % BSA and left to incubate for 3 h (5 % CO_2, 37 °C). Non-adherent cells were removed by washing the plate. Adherent cells were fixed and stained with crystal violet. Cell adhesion was then quantified by measuring the absorbance at 570 nm.

Wound healing experiments and histological examination

Studies in animal models were approved by the Ethical Committee of the San Raffaele Scientific Institute, and performed according to the prescribed guidelines. Littermates mice (75 % Sv129, 25 % C57BL/6 background, 7–8-week-old) were anesthetized with Avertine. The back of the mouse was shaved and sterilized using an alcohol swab. A sterile biopsy punch (Biopsy punch 8 mm, Huot Instruments) was used to punch through the full thickness of the back skin (two wounds/mouse). Proteins were diluted in 0.9 % sodium chloride solution and injected subcutaneously (2 µg/wounds) near the wound. The length and width of the wound were measured with a caliper. Skin samples (approximately 1–1.5 cm^2) containing the wound areas were collected at 2 and 9 days post-wounding and fixed in 4 % formaldehyde for histological analysis. Tissues were frozen and transversely cut into 10-µm-thick sections from the middle part of the wounds, stained with hematoxylin/eosin or immunostained with an anti-keratin 14 and with anti-Ki67 polyclonal antisera (1:500). For the Ki67 staining, tissues sections were heat-treated in 10 mM citrate buffer, pH 6, using a microwave (two cycles of 5 min). Antibody binding was detected using Alexa-Fluor-conjugated goat anti-rabbit IgG secondary antibody. Tissue sections were counterstained with DAPI and analyzed by fluorescence microscopy using an Axioscop 40FL microscope (Carl Zeiss, Germany) equipped with AxioCam MRc5 digital camera and Axiovison software (Carl Zeiss).

Results

Natural and recombinant CgA recognize the $\alpha v\beta 6$-integrin

The capability of natural and recombinant human chromogranin A (CgA and rCgA, respectively) to recognize various human integrins, including $\alpha v\beta 3$, $\alpha v\beta 5$, $\alpha v\beta 6$, $\alpha v\beta 8$, $\alpha 5\beta 1$, $\alpha 1\beta 1$, $\alpha 3\beta 1$, $\alpha 6\beta 4$, $\alpha 6\beta 7$ and $\alpha 9\beta 1$, was investigated by ELISA. In this assay CgA and rCgA, could recognize $\alpha v\beta 6$, but little or not at all the other integrins

(Fig. 1a). Both compounds could bind αvβ6 with a similar affinity (Fig. 1b), suggesting that protein glycosylation, which occurs only in natural CgA, was not crucial for the binding. Notably, the binding of CgA was detected either using an antibody against the $CgA_{68–71}$ epitope (mAb B4E11) (Fig. 1b), or using a polyclonal antibody against the $CgA_{410–439}$ epitope (Fig. 1c), data suggesting that full-length CgA could recognize αvβ6. Accordingly, Western-blot analysis of rCgA bound to αvβ6-coated microtiter plates showed a band of 70 kDa corresponding to intact CgA (Fig. 1d). Similar data were obtained with the N-terminal fragment of CgA (called vasostatin-1, VS-1) (Fig. 1a, b). These results suggest that both full-length CgA and N-terminal fragment VS-1 can bind the αvβ6 integrin.

The RGD site of CgA, residues 43–45, is necessary for αvβ6-integrin recognition

To assess the role of the RGD sequence of CgA (residues 43–45) in integrin recognition, we prepared a mutant of CgA carrying the $Asp_{45}Glu$ mutation, i.e., with RGE in place of RGD (therefore called rCgA–RGE). This change completely abolished the binding of CgA to αvβ6 (Fig. 1a), data suggesting that the RGD sequence of human CgA is critical for integrin recognition.

To further characterize the binding site of CgA, we performed competitive binding assays with a peptide containing the *iso*DGR motif, a mimetic of RGD known to bind various RGD-dependent integrins (which can be used, therefore, as a probe for the integrin binding site of various integrins) [31]. rCgA and VS-1 could compete the binding of the *iso*DGR-peptide to αvβ6 with similar potencies (Fig. 2a). In contrast, no inhibition was observed with the synthetic peptides $CgA_{1–40}$ and $CgA_{47–76}$, lacking RGD (Fig. 2a). Since we have previously shown that *iso*DGR binds within the RGD binding pocket of integrins [31, 32], these results suggest that also the RGD sequence of CgA can recognize this site. The competitive binding properties of VS-1 were completely abrogated by mAb 7D1 (against the RGD-containing region, residues 34–46), but not by mAb B4E11 and A11 (against residue 68–71 and 81–90, respectively) (Fig. 2b). Interestingly, the competitive binding properties of VS-1 were abrogated also by mAb 5A8 (against residues 54–57), suggesting that also the region adjacent to RGD is critical for the binding.

The region 38–63 of CgA, adjacent to RGD, is crucial for the selective recognition of αvβ6-integrin

To assess the contribution of the RGD-flanking regions in αvβ6-integrin recognition we then analyzed the binding properties of various fragments of CgA (see Supplementary Table 1S). A fragment encompassing the region 39–63 ($CgA_{39–63}$) could bind αvβ6 with an affinity 14-fold higher than that of CgA, whereas, a shorter peptide ($CgA_{38–47}$) was considerably less active (Table 1). These results suggest that the region 48–63, which contains an amphipathic α-helix [33], is very critical for the binding affinity. Accordingly, progressive deletion of the C-terminal residues from $CgA_{39–63}$ caused progressive loss of affinity (Table 1). In particular, a dramatic loss of activity was observed after removal of residues 47–59, adjacent to RGD. In contrast, $CgA_{39–59}$ and $CgA_{41–59}$ could recognize αvβ6 with similar affinity, suggesting that the residues that precede RGD are less critical. Furthermore, the peptide $CgA_{7–57}$ and $CgA_{39–57}$ could bind αvβ6 with similar affinities, indicating that the disulphide-bonded loop of CgA (residues 17–38) is not critical for binding.

While CgA and VS-1 could not recognize the integrins αvβ3, αvβ5, αvβ8 and α5β1 in the competition assay (even when tested at very high concentrations) $CgA_{39–63}$ could bind all these integrins, although with 200–1,000 lower affinity than αvβ6 (Table 1). Interestingly, $CgA_{38–47}$ (containing RGD and lacking α-helix and disulphide loop) could bind αvβ6 and αvβ3 with a K_i of 2,308 and 560 nM, respectively. These results, together, suggest that the RGD-flanking regions are very critical for binding affinity and selectivity.

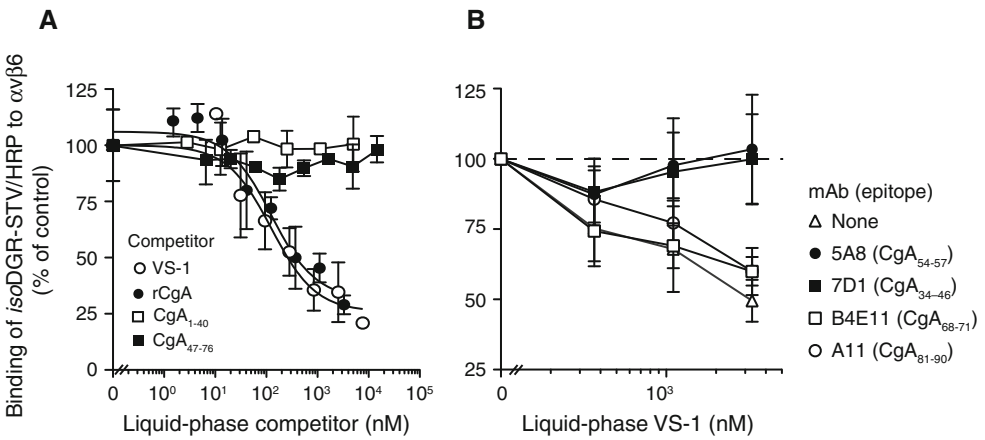

Fig. 2 The regions 41–46 and 54–57 of CgA are crucial for αvβ6 integrin recognition. **a** Binding competition of *iso*DGR/STV–HRP conjugate (a probe for the RGD site of αvβ6, [31]) with rCgA, VS-1, $CgA_{1–40}$ or $CgA_{47–76}$ to αvβ6. Representative experiment of three independent experiments (each in duplicate, mean ± SE). **b** Effect of various anti-CgA antibodies (100 μg/ml) on the competitive binding between *iso*DGR/STV–HRP and VS-1 to αvβ6

Table 1 Binding of CgA, VS-1 and various CgA-peptides to integrins as measured by competitive binding assay

Competitor	Binding of *iso*DGR-peptide									
	αvβ3		αvβ5		αvβ6		αvβ8		α5β1	
	(*n*)	K_i (nM)	(*n*)	K_i (nM)	(*n*)	K_i (nM)	(*n*)	K_i (nM)	(*n*)	K_i (nM)
rCgA	1	>2,000	1	>2,000	4	105 ± 34	1	>2,000	1	>2,000
VS-1	1	>10,000	1	>10,000	3	74 ± 30	1	>10,000	1	>10,000
$CgA_{38–47}$	1	561	1	10,282	2	2,308 ± 655	1	>30,000	1	5,886
$CgA_{38–53}$	2	3,104 ± 1,038	2	31,051 ± 12,410	3	104 ± 38	2	33,316 ± 818	1	6,655
$CgA_{38–57}$	1	3,051	1	26,566	4	86 ± 18	1	32,637		NA
$CgA_{38–59}$		NA		NA	3	31 ± 10		NA		NA
$CgA_{38–63}$		NA		NA	2	50 ± 26		NA		NA
$CgA_{38–63}$(RGE)		NA		NA	1	>50,000		NA		NA
$CgA_{39–57}$		NA		NA	2	41 ± 10		NA		NA
$CgA_{39–59}$	3	6,529 ± 1,475	2	18,901 ± 2,922	7	12 ± 0.01	3	27,243 ± 4,628	2	18,653 ± 404
$CgA_{39–61}$		NA		NA	3	19 ± 4		NA		NA
$CgA_{39–63}$	2	1,699 ± 522	2	4,855 ± 743	7	7.4 ± 4.4	2	7,394 ± 2,365	2	8,975 ± 2,672
$CgA_{39–64}$		NA		NA	3	16 ± 2		NA	1	>50,000
$CgA_{39–68}$(Y)	1	4,561	1	44,953	4	24 ± 8	1	30,443		NA
$CgA_{39–63}$(RGE)	1	>50,000	1	>50,000	1	>50,000	1	>50,000	1	>50,000
$CgA_{41–59}$	1	8,081	1	23,631	3	10 ± 5	1	39,775	1	22,661
$CgA_{7–47}$	1	3,705	1	24,440	2	>10,000	1	>30,000	1	17,025
$CgA_{7–53}$	1	10,706	1	28,629	2	136 ± 33	1	>30,000	1	>10,000
$CgA_{7–57}$	2	30,738 ± 12,555	1	>10,000	6	53 ± 11	1	>10,000	1	NA
A20FMVD2	1	12,518	1	16,201	4	0.6 ± 0.1	2	575 ± 540	2	1,015 ± 231
TP H2009.1	1	798	1	792	3	0.7 ± 0.3	2	342 ± 322	2	639 ± 199
Cilengitide	4	0.9 ± 0.1	5	0.8 ± 0.2	4	50 ± 25	4	121 ± 15	3	3 ± 1.4

n number of independent experiments (each in duplicate), K_i equilibrium dissociation constant of the competitor (mean ± SE). K_i was calculated by non-linear regression analysis of competitive binding data by using the "One site–Fit Ki" equation of the GraphPad Prism Software (GraphPad Software, Version 5.00 San Diego, California, USA), > maximum tested concentration, *NA* not analyzed, *cilengitide* cyclo(arginylglycyl-aspartyl-D-phenylalanyl-0*N*-methyl-valyl)

Comparison of $CgA_{39–63}$ with other RGD-containing integrin ligands

We then compared the integrin binding properties of $CgA_{39–63}$ with those of other peptides containing the RGD motif, such as cilengitide, A20FMDV2 and TPH2009.1, i.e., with peptides that are known to bind integrins with different affinity and selectivity [34–36]. All these peptides could bind αvβ6 and other integrins, such as αvβ3, αvβ5, αvβ8 and α5β1 (Table 1). However, the affinities of these peptides for the various integrins were markedly different. Of note, the binding pattern of $CgA_{39–63}$ was similar to that of A20FMDV2 and TPH2009.1 (which are selective for αvβ6) and distinct from that of cilengitide (which is more selective for αvβ3 and αvβ5) [35, 37].

Human CgA recognizes the αvβ6-integrin expressed by human and murine keratinocytes

To assess whether CgA can recognize αvβ6-integrin also when this receptor is expressed on the surface of living cells we have coupled $CgA_{38–63}$ to quantum dots ($CgA_{38–63}$-Qdot). In parallel, we prepared also a similar conjugate with RGD replaced with RGE [$CgA_{38–63}$(RGE)-Qdot]. The functional properties of both conjugates were first checked using purified αvβ6-integrin. As expected, $CgA_{38–63}$-Qdot, but not $CgA_{38–63}$(RGE)-Qdot, could bind αvβ6 in a dose-dependent manner (Fig. 3a). The binding of

Fig. 3 $CgA_{38–63}$ binds to αvβ6-integrin on HaCaT keratinocytes. ▶ **a** Binding of CgA38–63-Qdot, CgA38-63(RGE)-Qdot or Qdot to microtiter plates coated with αvβ6-integrin. The bound fluorescence was determined using a Victor Wallac3 instrument (excitation filter F355 nm, emission filter 595/60 nm). **b–d** Binding of $CgA_{38–63}$-Qdot, $CgA_{38–63}$(RGE)-Qdot or Qdot (1:30) to human HaCaT keratinocytes as measured by fluorescence microscopy and FACS. **c** Colocalization of $CgA_{38–63}$-Qdot binding and αvβ6 expression on HaCaT cell. HaCaT cell were incubated with $CgA_{38–63}$-Qdot (1:50, 2 h), washed and further incubated with anti-αvβ6 mAb 10D5 (5 μg/ml, 0.5 h, 37 °C) and ATTO 488-labeled goat anti-mouse IgGs. *Magnification* 630×, *red* Qdot, *blue* nuclear staining with DAPI, *green* ATTO 488. **e** Competitive binding of $CgA_{38–63}$-Qdot (1:30) to HaCaT cells with $CgA_{38–63}$ and $CgA_{38–63}$(RGE) (*left* and *middle*) or with anti-αvβ6 mAb 10D5 (10 μg/ml) (*right*), as measured by FACS

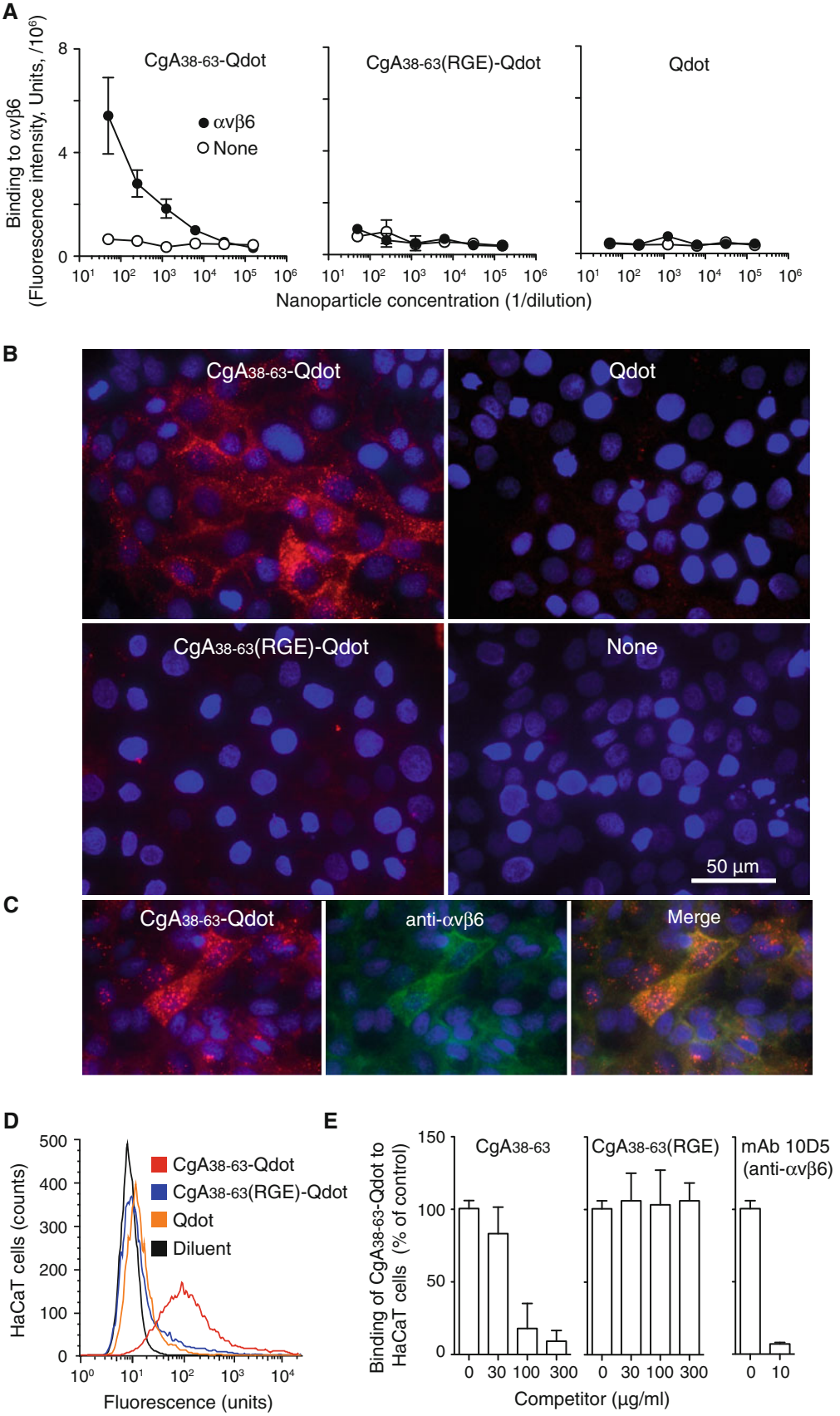
A
Binding to αvβ6 (Fluorescence intensity, Units, /10⁶)
CgA38-63-Qdot
CgA38-63(RGE)-Qdot
Qdot
αvβ6
None
Nanoparticle concentration (1/dilution)
B
CgA38-63-Qdot
Qdot
CgA38-63(RGE)-Qdot
None
50 µm
C
CgA38-63-Qdot
anti-αvβ6
Merge
D
HaCaT cells (counts)
CgA38-63-Qdot
CgA38-63(RGE)-Qdot
Qdot
Diluent
Fluorescence (units)
E
Binding of CgA38-63-Qdot to HaCaT cells (% of control)
CgA38-63
CgA38-63(RGE)
mAb 10D5 (anti-αvβ6)
Competitor (µg/ml)

these conjugates to HaCaT cells, a human keratinocyte cell line known to express αvβ6, was then investigated. Fluorescence microscopy analysis showed that $CgA_{38–63}$-Qdot, but not $CgA_{38–63}$(RGE)-Qdot, could bind these cells (Fig. 3b). Co-staining experiments with an anti-αvβ6 antibody (mAb 10D5) showed a good overlap between antibody binding and $CgA_{38–63}$-Qdot location (Fig. 3c). FACS analysis confirmed the RGD-dependent binding selectivity of these particles (Fig. 3d) and showed that an excess of free $CgA_{38–63}$, but not $CgA_{38–63}$(RGE), can inhibit the binding of $CgA_{38–63}$-Qdot to HaCaT cells (Fig. 3e, left and middle). The binding was totally inhibited also by an excess of mAb 10D5, a monoclonal antibody that is capable to block the active form of αvβ6 [38] (Fig. 3e, right). These results, together, suggest that the region $CgA_{38–63}$ of human CgA can bind, in an RGD-dependent manner, the αvβ6-integrin expressed on the cell membrane of human keratinocytes.

Remarkably, $CgA_{38–63}$-Qdot could also bind to murine keratinocytes (Supplementary Fig. 1S), suggesting that human CgA can recognize also murine αvβ6.

The RGD region of CgA can regulate the αvβ6-mediated adhesion of keratinocytes

The effect of the RGD region of CgA on the adhesion of keratinocyte to specific ligands was then investigated. Preliminary experiments showed that these cells, which express the αvβ6 and α6 integrins (Fig. 4a), can adhere to microtiter plates coated with anti-αvβ6 (mAb 10D5) or anti-α6 (mAb 135-13C) antibodies (Fig. 4b, left and middle). The addition of soluble $CgA_{39–63}$ to the cell culture inhibited the adhesion to anti-αvβ6, but not to anti-α6, antibody-coated plates (Fig. 4b, left and middle). Furthermore, $CgA_{39–63}$ inhibited keratinocyte adhesion to acetyl-C*iso*DGRCG peptide, a ligand of αvβ6 [31], but not to collagen-I (an adhesion molecule that does not recognize αvβ6) (Fig. 4b, right). AM20FMDV2 and $CgA_{39–63}$(RGE) were used as positive and negative controls (Fig. 4b, right). These results, suggest that the RGD site of CgA and its fragments can selectively regulate adhesion of keratinocytes mediated by αvβ6, but not the adhesion mediated by other integrins.

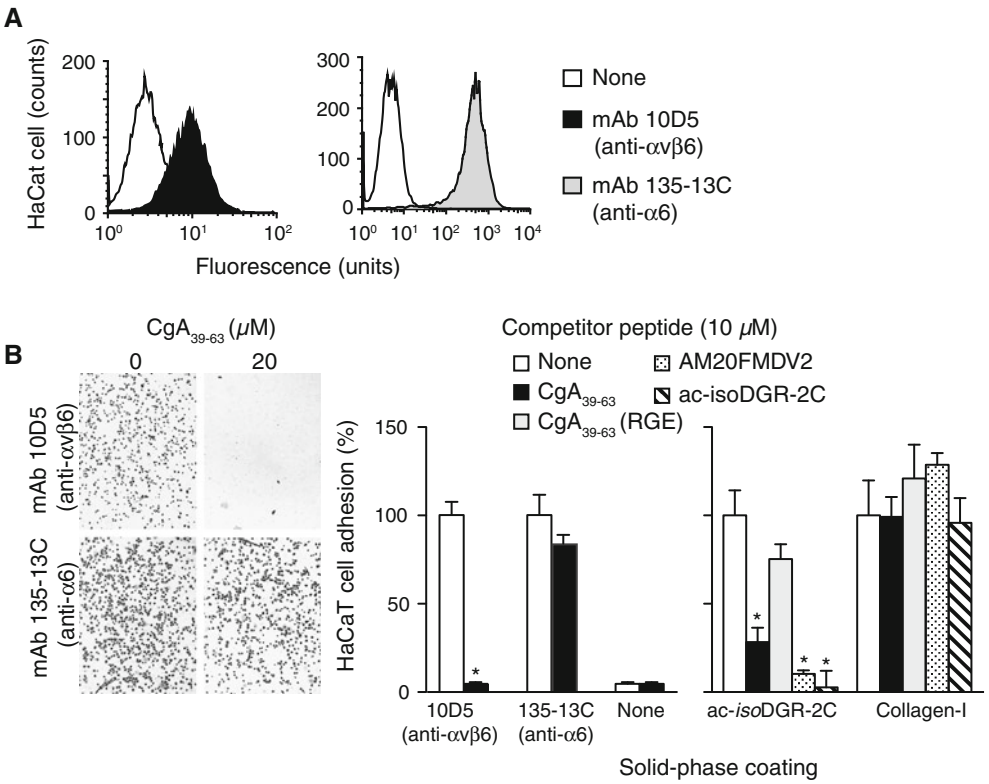

Fig. 4 RGD-dependent selective inhibition of αvβ6-mediated adhesion of keratinocytes by CgA-derived peptides. **a** Expression of αvβ6 and α6-integrin on HaCaT keratinocytes, as measured by FACS using the indicated monoclonal antibodies (10 μg/ml). **b** Effect of the indicated peptides on the adhesion of HaCaT cells to microtiter plates coated with 10D5 (an anti-αvβ6 mAb), 135-13C (an anti-α6 mAb), ac-*iso*DGR-2C (a peptide ligand of αvβ6) or collagen-I (an adhesion molecule that does not recognize αvβ6). The peptides were added to the cell supernatant before the adhesion assay. Microphotographs of HaCaT cell (100× *magnification*). The assay was performed as described in "Materials and methods". Mean ± SE ($n = 3$). *$p < 0.05$ statistical analysis by two-tailed *t* test

The role of CgA in cell adhesion and migration is further supported by the observation that the CgA N-terminal fragment VS-1, but not VS-1(RGE), could stimulate keratinocyte migration is a scratch closure assay (Supplementary Fig. 2S).

rCgA accelerates wound healing in vivo via RGD-dependent mechanisms

We then studied the effect of local injections of rCgA and rCgA–RGE on excisional wounds created on the back skin of mice. Fifty-percent reduction of the original wound area was observed after 2–3 days in mice treated with rCgA and after 5 days in mice treated with rCgA–RGE or diluent (Fig. 5a, left panels). Hematoxylin and eosin staining and immunofluorescence analysis of keratin-14 (a keratinocyte marker) of skin tissue sections obtained at day 2 showed a thicker epithelium in rCgA-treated mice than in controls (Fig. 5b). Furthermore, staining of Ki67 (a marker of cell proliferation) showed the presence of proliferating keratinocytes in the skin of CgA-treated mice (Fig. 5c). These results suggest that rCgA, exogenously administered, accelerates wound closure, and that the RGD-sequence plays a crucial role. Other in vivo studies performed with a similar dose (on a molar basis) of $CgA_{39–63}$ showed modest, non-significant, effects (Fig. 5a, right panels). Thus, besides RGD other sequences are likely important for the overall biological activity of CgA.

The RGD-sequence is replaced with QGD in murine CgA and is polymorphic in human CgA

Computer alignment of the sequences of CgA from different species showed that the region 39–63 is highly conserved among mammalian species, except for Arg_{43} that is replaced with Gln in mouse and rat (Fig. 6a). Thus, murine $CgA_{39–63}$ has QGD in place of RGD, whereas the rest of the sequence is 100 % conserved. Remarkably, a missense single-nucleotide polymorphism (SNP) that replaces Arg_{43} with Gln to generate QGD as in mice is present in the human population (http://www.ncbi.nlm.nih.gov/SNP/snp_ref.cgi?type=rs&rs=3742712).

In vitro αvβ6-binding studies showed that the QGD sequence was non-functional (data not shown) with potentially important functional implications for subjects bearing this SNP.

Discussion

The main finding of this work is that the RGD sequence of CgA (residues 43–45) can efficiently recognize the αvβ6 integrin. CgA binds to αvβ6 with high selectivity, as no binding was observed to other RGD-dependent and -independent integrins such as αvβ3, αvβ5, αvβ8, α5β1, α1β1, α3β1, α6β4, α6β7 and α9β1. Structure–activity studies performed with short fragments of CgA showed that the $CgA_{39–63}$ sequence is sufficient for high affinity binding to αvβ6 ($K_i = 7$ nM). Deletion of residues 47–63, known to form an amphipathic α-helix adjacent to RGD [33], caused a marked loss of affinity for αvβ6 and gain of affinity for other integrins. For example, while the $CgA_{39–63}$ fragment could recognize αvβ6 with an affinity 250–1,000-fold higher than that for αvβ3, αvβ5, αvβ8 and α5β1, deletion of the entire α-helix decreased the affinity for αvβ6 and markedly increased that for αvβ3. Thus, the amphipathic α-helix adjacent to RGD is crucial for both binding affinity and selectivity.

These structural elements (i.e., RGD followed by an amphipathic α-helix) are present also in other peptides (called AM20FMDV2, A20LAP) previously described by other investigators as selective ligands of αvβ6 [37]. The sequences of AM20FMDV2 and A20LAP peptide correspond to the VP1 coat protein of the foot-and-mouth disease virus and of the latency-associated peptide of transforming growth factor-β1, respectively. Similar to CgA, also the α-helix of these peptides is crucial for αvβ6-binding affinity and selectivity. It has been proposed that the RGDLXXL/I sequence, which is common to these peptides (see Fig. 6a), is a consensus motif for the selective binding to αvβ6 [37, 40, 41]. Considering that CgA has a Glu residue after RGD, instead of Leu (Fig. 6a), the consensus motif appears to be RGDE/LXXL/I.

Another important finding of this work is that human CgA can regulate the physiology of keratinocytes and accelerate the wound healing process via RGD-dependent mechanisms. This hypothesis is supported by the observation that replacement of RGD with RGE in human CgA abolishes its activity in several in vitro and in vivo assays involving human and murine keratinocytes. It is tempting to speculate that the activity of CgA on keratinocytes is mediated by this site. However, we cannot exclude that besides RGD other sequences of CgA play a role in the wound healing.

How does CgA accelerate wound healing? Previous studies in humans and animals have shown that β6 mRNA is detectable in keratinocytes at the wound edge [42, 43]. Furthermore, that the integrin αvβ6 is up-regulated in skin epidermis during wound healing [39] and plays important roles in keratinocyte migration, TGF-β1 maturation, regeneration of basement membrane, regulation of inflammatory reaction and formation of granulation tissue [25]. Other in vitro studies have shown that αvβ6 promotes keratinocyte adhesion and migration on components of the wound matrix, such as fibronectin, tenascin and vitronectin [43–45]. Given the high selectivity of CgA for αvβ6 and

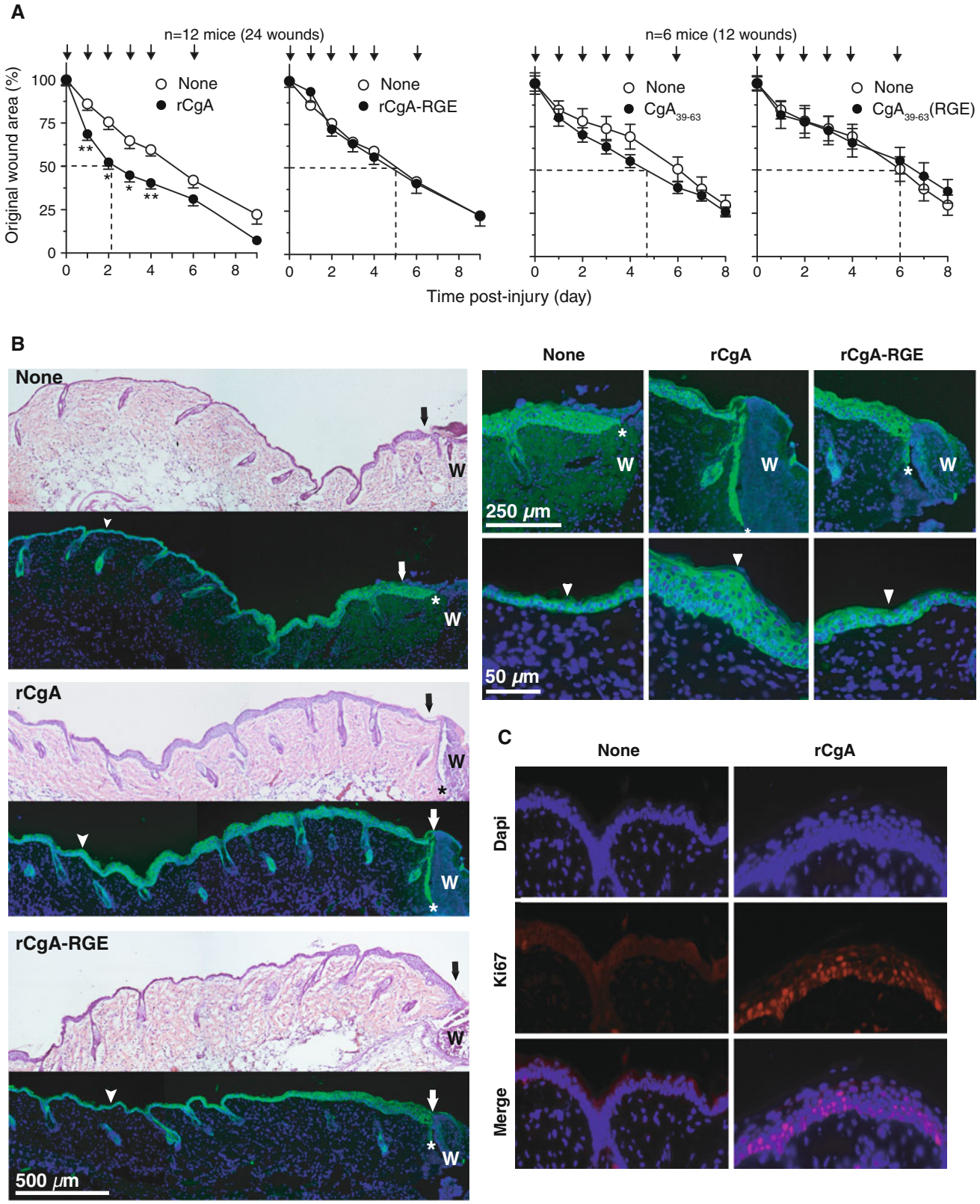

the crucial role of the RGD sequence of CgA in wound healing experiments, we speculate that the RGD site of CgA contributes to regulate the function of this integrin in keratinocyte adhesion and migration during wound healing. This hypothesis is supported by the results of adhesion assays showing that HaCat keratinocytes adhesion to

◄ **Fig. 5** RGD-dependent acceleration of wound healing in mice by CgA. **a** Effect of rCgA, rCgA–RGE, $CgA_{38–63}$ and $CgA_{38–63}$(RGE) on skin wound healing in mice. Each product was injected subcutaneously around the wound (40 pmol/wound, two wounds/mouse) at the indicated time (*arrows*). $^{**}p < 0.01$, $^{*}p < 0.05$ by two-tailed *t* test. **b**, **c** Histochemical analysis of skin tissue sections at day 2. The epidermis adjacent to the wound (*W*) is shown. Tissue sections were stained with hematoxylin and eosin, anti-keratin-14 or anti-Ki67 proliferation marker antibodies (*green* keratin-14, *red* Ki67, *blue* nuclear staining with DAPI). In *panel B*, *left*, two-adjacent fields were photographed (100× or 400× *magnification*, digitally enlarged and assembled using Adobe Photoshop. *Arrows* indicate the original margin of the wound, *asterisks* indicate the position of the advancing epithelial edges, *arrowheads* indicate the enlarged regions showing a thicker epithelium in CgA-treated mice

ligands of αvβ6, but not to ligands of other integrins (e.g., collagen I), is inhibited by $CgA_{39–63}$ and that this effect is again abolished by replacement of RGD with RGE. Moreover, VS-1, but not VS-1(RGE) could increase keratinocyte migration in vitro (Supplementary Fig. 2S). The functional role of the RGD site of CgA as a modulator of keratinocyte physiology is further supported by the results of immunohistological analysis of skin tissue section obtained from injured mice, showing that rCgA, but not rCgA-RGE, could induce thickening of epidermis. Staining of skin tissue sections with an anti-Ki67 antibody (a cell proliferation marker) showed that rCgA could increase keratinocyte proliferation. Thus, we propose that CgA might accelerate wound healing by affecting keratinocyte adhesion, proliferation and migration and that the RGD/αvβ6 interactions are important for this activity. However, the observation that a $CgA_{39–63}$ peptide is less potent than CgA in wound healing experiments, despite its good affinity for αvβ6, suggest that other receptors implicating non-RGD sequences of CgA are also involved.

Interestingly, the region 39–63 of CgA is highly conserved among different mammalian species, except for Arg_{43} that is replaced with Gln in mouse and rat (Fig. 6a). Furthermore, a missense single-nucleotide polymorphism that generates QGD is present in the human population. The results of in vitro binding assays show that the RGD sequence is necessary for binding and that the QGD-alpha-helix region is non-functional. One possible important

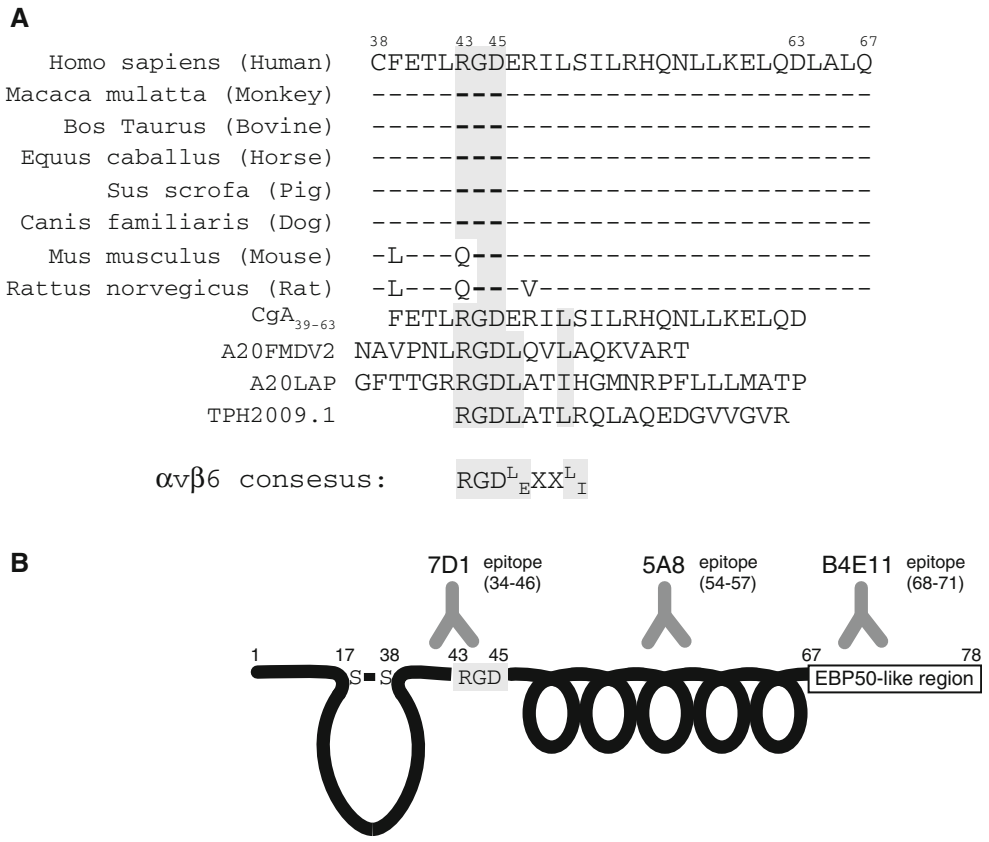

Fig. 6 Alignment of the CgA sequences from different species with RGD peptides selective for αvβ6. **a** The peptide AM20FMDV2 is derived from the foot-and-mouth disease virus; the A20LAP peptide was derived from the latency-associated peptide of transforming growth factor-β1; the TP H2009.1 peptide was identified by phage-display screening on H2009.1 cell expressing αvβ6. The consensus motif is also shown. Note that RGD is replaced with QGD in mouse and rat CgA. **b** Schematic representation of the N-terminal domain of CgA showing the RGD motif and the amphipathic α-helix. Antibody epitope topography and ezrin-binding-protein-50-homology domain [15–18] are also indicated. mAb 7D1 and 5A8, but not B4E11 can block the CgA/αvβ6 interaction

implication of our findings is that individuals that have QGD in place of RGD have lower wound healing rates. Regarding rodents, it is interesting to note that rats have an RGD sequence in the C-terminal region. However, the functional role of this region is presently unknown.

This raises the question as to whether the missense single-nucleotide polymorphism present in the human population can affect the wound healing rate, which may have important pathophysiological implications.

Previous studies performed with antibodies against the mouse CgA region 364–384 showed that CgA is overexpressed in wound keratinocytes [3]. We confirmed this observation using an antibody against CgA 54–57 (Supplementary Fig 3S). The overexpression of these epitopes may suggest that murine CgA plays some other useful functions, despite it lacks RGD. For example, it has been proposed that CgA, being a precursor of several peptides with antibacterial and antifungal activity, might play a role in innate immunity in the skin [3].

In conclusion, the results of the present study show that human CgA can regulate the physiology of keratinocytes and the wound healing process in mice through an RGD-dependent mechanism, likely involving the $\alpha v\beta 6$-integrin. Since this integrin is expressed also by neoplastic epithelial cells, these results may stimulate further studies aimed at assessing the role of CgA and $\alpha v\beta 6$ in cancer.

Acknowledgments This work was supported by Associazione Italiana per la Ricerca sul Cancro (AIRC 9965 and 9180), and Alleanza Contro il Cancro (ACC) of Italy.

Conflict of interest The authors declare no conflicts of interest.

References

1. Helle KB, Corti A, Metz-Boutigue MH, Tota B (2007) The endocrine role for chromogranin A: a prohormone for peptides with regulatory properties. Cell Mol Life Sci 22:2863–2886
2. Corti A (2010) Chromogranin A and the tumor microenvironment. Cell Mol Neurobiol 8:1163–1170
3. Radek KA, Lopez-Garcia B, Hupe M, Niesman IR, Elias PM, Taupenot L, Mahata SK, O'Connor DT, Gallo RL (2008) The neuroendocrine peptide catestatin is a cutaneous antimicrobial and induced in the skin after injury. J Invest Dermatol 6:1525–1534
4. Gayen JR, Saberi M, Schenk S, Biswas N, Vaingankar SM, Cheung WW, Najjar SM, O'Connor DT, Bandyopadhyay G, Mahata SK (2009) A novel pathway of insulin sensitivity in chromogranin A null mice: a crucial role for pancreastatin in glucose homeostasis. J Biol Chem 42:28498–28509
5. Gonzalez-Yanes C, Sanchez-Margalet V (2003) Pancreastatin, a chromogranin A-derived peptide, inhibits leptin and enhances UCP-2 expression in isolated rat adipocytes. Cell Mol Life Sci 12:2749–2756
6. Mahata SK, Mahata M, Fung MM, O'Connor DT (2010) Catestatin: a multifunctional peptide from chromogranin A. Regul Pept 1–3:33–43
7. Mahata SK, O'Connor DT, Mahata M, Yoo SH, Taupenot L, Wu H, Gill BM, Parmer RJ (1997) Novel autocrine feedback control of catecholamine release. A discrete chromogranin a fragment is a noncompetitive nicotinic cholinergic antagonist. J Clin Invest 6:1623–1633
8. Mahata SK, Mahata M, Parmer RJ, O'Connor DT (1999) Desensitization of catecholamine release. The novel catecholamine release-inhibitory peptide catestatin (chromogranin a344–364) acts at the receptor to prevent nicotinic cholinergic tolerance. J Biol Chem 5:2920–2928
9. Tota B, Angelone T, Mazza R, Cerra MC (2008) The chromogranin A-derived vasostatins: new players in the endocrine heart. Curr Med Chem 14:1444–1451
10. Lugardon K, Raffner R, Goumon Y, Corti A, Delmas A, Bulet P, Aunis D, Metz-Boutigue MH (2000) Antibacterial and antifungal activities of vasostatin-1, the N-terminal fragment of chromogranin A. J Biol Chem 275:10745–10753
11. Eskeland NL, Zhou A, Dinh TQ, Wu H, Parmer RJ, Mains RE, O'Connor DT (1996) Chromogranin A processing and secretion: specific role of endogenous and exogenous prohormone convertases in the regulated secretory pathway. J Clin Invest 1:148–156
12. Doblinger A, Becker A, Seidah NG, Laslop A (2003) Proteolytic processing of chromogranin A by the prohormone convertase PC2. Regul Pept 1–3:111–116
13. Colombo B, Curnis F, Foglieni C, Monno A, Arrigoni G, Corti A (2002) Chromogranin A expression in neoplastic cells affects tumor growth and morphogenesis in mouse models. Cancer Res 3:941–946
14. Biswas N, Rodriguez-Flores JL, Courel M, Gayen JR, Vaingankar SM, Mahata M, Torpey JW, Taupenot L, O'Connor DT, Mahata SK (2009) Cathepsin L colocalizes with chromogranin A in chromaffin vesicles to generate active peptides. Endocrinology 8:3547–3557
15. Gasparri A, Sidoli A, Sanchez LP, Longhi R, Siccardi AG, Marchisio PC, Corti A (1997) Chromogranin A fragments modulate cell adhesion. Identification and characterization of a pro-adhesive domain. J Biol Chem 33:20835–20843
16. Ratti S, Curnis F, Longhi R, Colombo B, Gasparri A, Magni F, Manera E, Metz-Boutigue MH, Corti A (2000) Structure–activity relationships of chromogranin A in cell adhesion. Identification and characterization of an adhesion site for fibroblasts and smooth muscle cells. J Biol Chem 38:29257–29263
17. Colombo B, Longhi R, Marinzi C, Magni F, Cattaneo A, Yoo SH, Curnis F, Corti A (2002) Cleavage of chromogranin A N-terminal domain by plasmin provides a new mechanism for regulating cell adhesion. J Biol Chem 48:45911–45919
18. Dondossola E, Gasparri A, Bachi A, Longhi R, Metz-Boutigue MH, Tota B, Helle KB, Curnis F, Corti A (2010) Role of vasostatin-1 C-terminal region in fibroblast cell adhesion. Cell Mol Life Sci 12:2107–2118
19. Ferrero E, Magni E, Curnis F, Villa A, Ferrero ME, Corti A (2002) Regulation of endothelial cell shape and barrier function by chromogranin A. Ann N Y Acad Sci 971:355–358
20. Ferrero E, Scabini S, Magni E, Foglieni C, Belloni D, Colombo B, Curnis F, Villa A, Ferrero ME, Corti A (2004) Chromogranin A protects vessels against tumor necrosis factor alpha-induced vascular leakage. FASEB J 3:554–556
21. Belloni D, Scabini S, Foglieni C, Veschini L, Giazzon A, Colombo B, Fulgenzi A, Helle KB, Ferrero ME, Corti A, Ferrero E (2007) The vasostatin-I fragment of chromogranin A inhibits VEGF-induced endothelial cell proliferation and migration. FASEB J 12:3052–3062

22. Plow EF, Haas TA, Zhang L, Loftus J, Smith JW (2000) Ligand binding to integrins. J Biol Chem 29:21785–21788
23. Humphries JD, Byron A, Humphries MJ (2006) Integrin ligands at a glance. J Cell Sci 119(Pt 19):3901–3903
24. Barczyk M, Carracedo S, Gullberg D (2010) Integrins. Cell Tissue Res 1:269–280
25. Thomas GJ, Nystrom ML, Marshall JF (2006) Alphavbeta6 integrin in wound healing and cancer of the oral cavity. J Oral Pathol Med 1:1–10
26. Curnis F, Gasparri A, Sacchi A, Cattaneo A, Magni F, Corti A (2005) Targeted delivery of IFNgamma to tumor vessels uncouples antitumor from counterregulatory mechanisms. Cancer Res 7:2906–2913
27. D'Alessio S, Gerasi L, Blasi F (2008) uPAR-deficient mouse keratinocytes fail to produce EGFR-dependent laminin-5, affecting migration in vivo and in vitro. J Cell Sci 121(Pt 23): 3922–3932
28. Corti A, Longhi R, Gasparri A, Chen F, Pelagi M, Siccardi AG (1996) Antigenic regions of human chromogranin A and their topographic relationships with structural/functional domains. Eur J Biochem 235(1–2):275–280
29. Corti A, Sanchez LP, Gasparri A, Curnis F, Longhi R, Brandazza A, Siccardi AG, Sidoli A (1997) Production and structure characterisation of recombinant chromogranin A N-terminal fragments (vasostatins)—evidence of dimer–monomer equilibria. Eur J Biochem 3:692–699
30. Fields GB, Noble RL (1990) Solid phase peptide synthesis utilizing 9-fluorenylmethoxycarbonyl amino acids. Int J Pept Protein Res 3:161–214
31. Curnis F, Cattaneo A, Longhi R, Sacchi A, Gasparri AM, Pastorino F, Di Matteo P, Traversari C, Bachi A, Ponzoni M, Rizzardi GP, Corti A (2010) Critical role of flanking residues in NGR-to-isoDGR transition and CD13/integrin receptor switching. J Biol Chem 12:9114–9123
32. Spitaleri A, Mari S, Curnis F, Traversari C, Longhi R, Bordignon C, Corti A, Rizzardi GP, Musco G (2008) Structural basis for the interaction of isoDGR with the RGD-binding site of alphavbeta3 integrin. J Biol Chem 28:19757–19768
33. Lugardon K, Chasserot-Golaz S, Kieffer AE, Maget-Dana R, Nullans G, Kieffer B, Aunis D, Metz-Boutigue MH (2001) Structural and biological characterization of chromofungin, the antifungal chromogranin A-(47–66)-derived peptide. J Biol Chem 38:35875–35882
34. Dechantsreiter MA, Planker E, Matha B, Lohof E, Holzemann G, Jonczyk A, Goodman SL, Kessler H (1999) N-Methylated cyclic RGD peptides as highly active and selective alpha(V)beta(3) integrin antagonists. J Med Chem 16:3033–3040
35. Elayadi AN, Samli KN, Prudkin L, Liu YH, Bian A, Xie XJ, Wistuba II, Roth JA, McGuire MJ, Brown KC (2007) A peptide selected by biopanning identifies the integrin alphavbeta6 as a prognostic biomarker for nonsmall cell lung cancer. Cancer Res 12:5889–5895
36. Hausner SH, DiCara D, Marik J, Marshall JF, Sutcliffe JL (2007) Use of a peptide derived from foot-and-mouth disease virus for the noninvasive imaging of human cancer: generation and evaluation of 4-[18F]fluorobenzoyl A20FMDV2 for in vivo imaging of integrin alphavbeta6 expression with positron emission tomography. Cancer Res 16:7833–7840
37. DiCara D, Rapisarda C, Sutcliffe JL, Violette SM, Weinreb PH, Hart IR, Howard MJ, Marshall JF (2007) Structure-function analysis of Arg-Gly-Asp helix motifs in alpha v beta 6 integrin ligands. J Biol Chem 13:9657–9665
38. Huang X, Wu J, Spong S, Sheppard D (1998) The integrin alphavbeta6 is critical for keratinocyte migration on both its known ligand, fibronectin, and on vitronectin. J Cell Sci 111:2189–2195
39. Breuss JM, Gallo J, DeLisser HM, Klimanskaya IV, Folkesson HG, Pittet JF, Nishimura SL, Aldape K, Landers DV, Carpenter W et al (1995) Expression of the beta 6 integrin subunit in development, neoplasia and tissue repair suggests a role in epithelial remodeling. J Cell Sci 108:2241–2251
40. Logan D, Abu-Ghazaleh R, Blakemore W, Curry S, Jackson T, King A, Lea S, Lewis R, Newman J, Parry N et al (1993) Structure of a major immunogenic site on foot-and-mouth disease virus. Nature 6420:566–568
41. Kraft S, Diefenbach B, Mehta R, Jonczyk A, Luckenbach GA, Goodman SL (1999) Definition of an unexpected ligand recognition motif for alphav beta6 integrin. J Biol Chem 4:1979–1985
42. Clark RA, Ashcroft GS, Spencer MJ, Larjava H, Ferguson MW (1996) Re-epithelialization of normal human excisional wounds is associated with a switch from alpha v beta 5 to alpha v beta 6 integrins. Br J Dermatol 1:46–51
43. Hakkinen L, Hildebrand HC, Berndt A, Kosmehl H, Larjava H (2000) Immunolocalization of tenascin-C, alpha9 integrin subunit, and alphavbeta6 integrin during wound healing in human oral mucosa. J Histochem Cytochem 7:985–998
44. Busk M, Pytela R, Sheppard D (1992) Characterization of the integrin alpha v beta 6 as a fibronectin-binding protein. J Biol Chem 9:5790–5796
45. Koivisto L, Larjava K, Hakkinen L, Uitto VJ, Heino J, Larjava H (1999) Different integrins mediate cell spreading, haptotaxis and lateral migration of HaCaT keratinocytes on fibronectin. Cell Adhes Commun 3:245–257